# Electrospun formulations of acyclovir, ciprofloxacin and cyanocobalamin for ocular drug delivery

Alexandra Baskakova,[1,2,†] Sahar Awwad,[2,†] Jennifer Quirós Jiménez,[2,3] Hardyal Gill,[2] Oleg Novikov,[1] Peng T. Khaw,[4] Steve Brocchini,[2] Elena Zhilyakova,[1,*] Gareth R. Williams[2,*]

1. Department of Pharmaceutical Technology, Belgorod State University, 85 Pobeda Street, Belgorod, 308001, Russia
2. UCL School of Pharmacy, University College London, 29 – 39 Brunswick Square, London, WC1N 1AX, UK.
3. Department of Chemical Engineering, University of Alcalá, E-28871 Alcalá de Henares, Madrid, Spain.
4. NIHR Biomedical Research Centre, Moorfields Eye Hospital and UCL Institute of Ophthalmology, London, EC1V 9EL, UK

* Authors for correspondence. Email: ezhilyakova@bsu.edu.ru (EZ); g.williams@ucl.ac.uk (GRW); Tel: +7 (4722) 301 427 (EZ); +44 (0) 207 753 5868 (GRW).

† These authors contributed equally to this work.

## Abstract

Two series of fibers containing the active ingredients acyclovir, ciprofloxacin and cyanocobalamin, and combinations of these drugs, were prepared by electrospinning. One set used the hydrophilic poly(vinylpyrrolidone) (PVP) as the filament-forming polymer, while the other used the slow-dissolving poly(ε-caprolactone) (PCL). The fibers were found to have cylindrical morphologies, although there was evidence for solvent occlusion with the PVP systems and for some drug particles in the PCL case. The active ingredients were generally present in the amorphous physical form in the case of PVP, but evidence of crystallinity was observed with PCL. The existence of intermolecular interactions between the drugs and polymers was proven using simple molecular modeling calculations. Drug release from the various fibers was tested in a validated *in vitro* outflow model of the eye, and the fiber formulations found to be capable of extending drug release. We thus conclude that electrospun matrices such as those prepared in this work have potential for use as intravitreal implants.



## Keywords

Electrospinning, ocular drug delivery, *in vitro*, half-life, antivirals, posterior segment, fibers, sustained release.


## Chemical compounds used in this work

Acyclovir (Pubchem ID: 2022); ciprofloxacin (2764); cyanocobalamin (5311498).

## 1. Introduction

Cytomegalovirus (CMV) infections are a major clinical problem in patients with AIDS. Their main manifestation in AIDS patients is retinitis, which accounts for 20-30% of all cases (Pollard, 1996). Common symptoms of CMV retinitis include visual field defects with decreased acuity, the presence of floaters, and photophobia. Complications arise when retinitis is localized near the macula, which can lead to loss of vision and to hemorrhages replaced eventually by thin atrophic scar tissue and inflammation (Jouan and Katlama, 1999). Most ocular drugs when given by topical administration are rapidly cleared by the aqueous humor flowing into the anterior chamber and flushing the drug out via the trabecular meshwork, should they permeate the cornea. The drug will often therefore fail to reach reproducible therapeutic levels near the retina (Haghjou et al., 2013). Intravitreal (IVT) injection can provide adequate drug concentrations in the posterior segment. Unfortunately drugs in solution can rapidly clear within hours from the posterior cavity upon IVT injection. This reduces efficacy and frequent injections are required, which can lead to undesirable side effects, and reduce patient compliance (Short, 2008).

To solve the general problem of fast ocular clearance times, new strategies are being investigated to deliver drugs as intravitreal implants specifically designed to prolong release. One example is Vitrasert® (Bausch & Lomb Inc, Rochester, NY, USA), a ganciclovir loaded intravitreal implant approved by the US Food and Drug Administration and administered for the treatment of CMV retinitis. The implant is primarily made of ethylene-vinyl acetate and polyvinyl alcohol, and the drug is released over a period of 6-8 months (Kuno and Fujii, 2011).

There are a number of drug candidates that can be used to treat ocular infections. Acyclovir (ACY) is an effective antiviral agent but is only slightly soluble in water. This limits its use in the

eye since it is challenging to prepare a solution with sufficient solubility to exert a therapeutic effect. Ciprofloxacin (CIP) is widely used to prevent and cure bacterial infections, and thus can be used with ACY to provide broad-spectrum anti-pathogenic activity. It too has very poor water solubility. Cyanocobalamin (vitamin B12) has been reported to repair damage to the eye, and is used as a reparative agent in some eye drops (*e.g.* Sante Beautéye (Santen Pharmaceutical Co, 2013)). A formulation containing all three ingredients, with solubility enhancement for ACY and CIP, would thus be a useful addition to the gamut of treatments for viral diseases of the eye.

Various strategies can be applied to increase the solubility and dissolution rate of poorly soluble drugs; one popular approach is to prepare amorphous dispersions of the active pharmaceutical ingredient (API) in a polymer matrix. The formation of such a solid solution or solid suspension removes the lattice energy barrier to dissolution, and the polymer carrier additionally helps to stabilize the amorphous form by preventing the API molecules from crystallizing. One method which has been widely explored to generate such pharmaceutical composites is electrospinning (Chakraborty et al., 2009; Williams et al., 2012). This approach is attractive in its simplicity. A co-dissolving solution of a polymer and an API is first prepared in a volatile solvent. This is then loaded into a syringe fitted with a metal needle (the spinneret). The polymer solution is ejected from the syringe towards a metal collector plate at a constant rate, controlled using a syringe pump. A high potential difference is applied between the spinneret (positive) and collector (grounded), causing rapid evaporation of the solvent and the formation of a non-woven mesh of polymer/API fibers, often with dimensions on the nanoscale.

Electrospinning has been used to prepare numerous formulations with enhanced solubility/dissolution characteristics, and ACY, CIP and B12 have all been previously processed

in this manner. Only a single publication relating to B12 electrospinning could be found in the literature, focused on preparing temperature-sensitive release systems based on poly(ethylene oxide) and poly(isopropylacrylamide) (Song et al., 2011). A number of reports of CIP spinning exist, focused primarily on would dressings (El-Shanshory et al., 2015; Unnithan et al., 2012), oral hygiene (Bottino et al., 2014) or urinary devices (Macocinschi et al., 2015): no studies have been reported targeted at ocular drug delivery.

Yu et al. have undertaken several investigations into ACY fibers, using both slow and fast dissolving polymers. Core/shell fibers of poly(vinyl pyrrolidone) (PVP) were prepared with a shell containing PVP, sodium dodecyl sulfate (as a permeation enhancer) and sucralose (a flavor enhancer), and a PVP/ACY core (Yu et al., 2011). These were designed for oral application, and found to release all the incorporated drug within 1 minute. Analogous systems and results were obtained using electrospraying, a technique closely related to electrospinning which produces particles instead of fibers (Liu et al., 2014). Sustained release systems loaded with ACY have also been prepared with poly(acrylonitrile) as the carrier polymer (Chen and Yu, 2010; Yu et al., 2010).

All of the abovementioned systems were prepared with applications other than the ocular field in mind. In this work, we sought to develop electrospun systems to allow effective healing of viral eye infections. ACY, CIP and B12 (see Figure 1) were first spun individually before combination formulations were prepared. In order to explore drug release in a representative environment, functional performance assays were performed using the recently reported PK-Eye model (Awwad et al., 2015), depicted in Figure 2. This aims to provide a reliable *in vitro* proxy for drug dissolution and distribution in the eye. There is no model for the eye given in the pharmacopoeia, and the few *in vitro* models reported in the literature are limited in that they

do not mimic the human eye in terms of scale and/or mass transfer. While *in vitro* models are of course not completely representative of what occurs *in vivo*, they are widely used in formulation to predict *in vivo* performance. The PK-Eye is currently being used to *develop in vitro – in vivo* correlations for ocular formulations and the use of this model avoids the use of animals, which are not generally predictive of human ocular pharmacokinetics. To plot a reliable time-concentration curve for ocular pharmacokinetics at least 36 rabbits would be required, which is unacceptable for drug screening and inconsistent with the 3Rs philosophy. The PK-Eye is specifically designed as a two-compartment model scaled to human dimensions and mimics the intraocular aqueous outflow through the anterior route. In this study, the API-loaded fibers were tested in the posterior cavity of the PK-Eye to observe their release behavior.

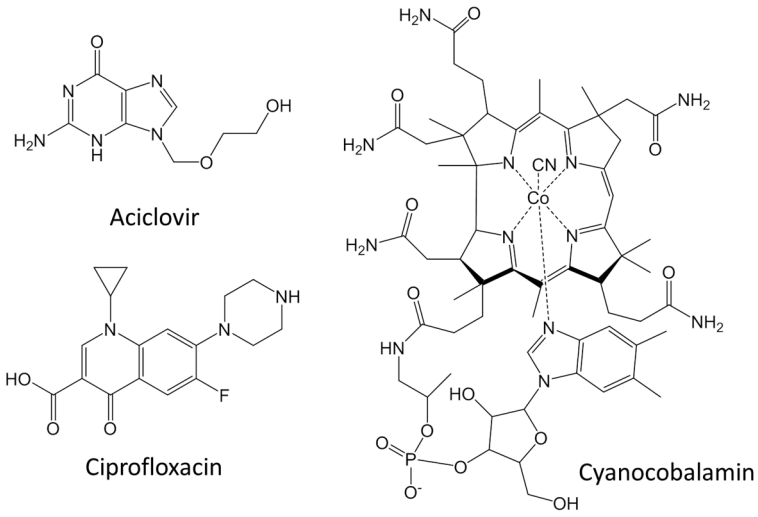


**Figure 1:** The chemical structures of acyclovir, ciprofloxacin and cyanocobalamin.

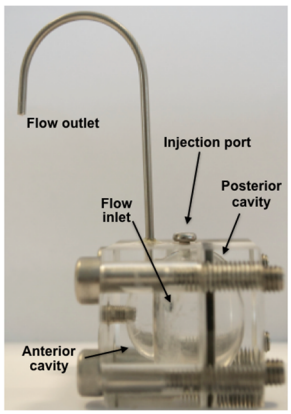


**Figure 2:** The PK-Eye model. Adapted from Awwad et al. 2015.

# 2. Experimental section

## 2.1 Materials

Polyvinylpyrrolidone K60 (PVP; molecular weight 360,000 Da), polycaprolactone (PCL; molecular weight 70,000 Da), acyclovir (ACY), ciprofloxacin (CIP), chloroform, and N,N-dimethylformamide (DMF) were procured from Sigma-Aldrich (Gillingham, UK), while cyanocobalamin (vitamin B12) and methanol (AR grade) were sourced from Fisher Scientific (Loughborough, UK).

## 2.2 Electrospinning

Solutions for electrospinning (ES) were prepared by dissolving the required amount of drug and polymer in DMF/chloroform (for PVP fibers; 1:1 v/v) or chloroform/methanol (for PCL fibers; 1:1 v/v). The API was added to 10 mL of solvent in a clear glass vial and stirred at room temperature (RT) for *ca.* 2 h until complete dissolution was achieved. After this, 1900 mg PVP or 750 mg PCL was slowly added and the resultant solutions stirred overnight at RT. During stirring, the glass vials were sealed with a rubber cup to avoid solvent evaporation.

For ES, the API/polymer solution was loaded into a 5 mL plastic syringe to which a stainless steel needle (spinneret; 18G, internal diameter 0.84 mm; Nordson EFD, Dunstable, UK) was attached. A high voltage DC power supply (HCP 35-35,000, FuG Electronic, Rosenheim, Germany) was employed to provide a high voltage between the spinneret and a metal collector plate. For all experiments, the applied voltage was 12 kV, the spinneret-to-collector distance 15 cm and the flow rate 0.5 mL $h^{-1}$. All processes were conducted at ambient temperature and pressure (22 ± 3 °C, and 30 ± 5 % relative humidity). After manufacturing, samples were wrapped in aluminum foil and stored in a desiccator for at least 12 h prior to analysis. Silica gel was used as desiccant, maintaining the relative humidity inside the desiccator below 25 %. Details of the spinning solutions prepared and the resultant fiber compositions are given in Table 1.

**Table 1:** Details of the spinning solutions and fibers prepared.

| Polymer | Drug | Formulation ID | Polymer conc in solution (% w/v) | API conc in solution (% w/v) | Polymer conc in fibers (% w/w) | API conc in fibers (% w/w) |
|---|---|---|---|---|---|---|
| PVP | ACY | PVP-ACY | 19 | 1 | 95 | 5 |
| | CIP | PVP-CIP | 19 | 0.3 | 98.4 | 1.6 |
| | B12 | PBP-B12 | 19 | 0.2 | 99.0 | 1.0 |
| | ACY | PVP-ABC | 19 | 1 | 92.7 | 4.9 |
| | B12 | | | 0.3 | | 1.5 |
| | CIP | | | 0.2 | | 1.0 |
| PCL | ACY | PCL-ACY | 7.5 | 1 | 88.2 | 11.8 |
| | CIP | PCL-CIP | 7.5 | 0.3 | 96.2 | 3.8 |
| | B12 | PCL-B12 | 7.5 | 0.2 | 97.4 | 2.6 |
| | ACY -CIP | PCL-AC | 7.5 | 1 | 85.2 | 11.4 |
| | | | | 0.3 | | 3.4 |
| | ACY-B12-CIP | PCL-ABC | 7.5 | 1 | 83.3 | 11.1 |
| | | | | 0.3 | | 3.3 |
| | | | | 0.2 | | 2.2 |

## 2.3 Characterization

### *2.3.1 Scanning electron microscopy*

Scanning electron microscopy (SEM) was used to investigate the morphology of the fibers prepared. Samples were cut from the fiber mats and adhered onto aluminium SEM stubs using carbon-coated double-sided tape. In order to make them electrically conductive, they were then sputter coated with gold prior to imaging. Images were obtained using a Quanta 200F instrument (FEI, Hillsboro, OR, USA). The fiber diameter was determined with the aid of the ImageJ software (National Institutes of Health, Bethesda, MD, USA): at least 50 fibers were measured, and the results are reported as mean ± S.D.

### *2.3.2 Differential scanning calorimetry*

Differential Scanning Calorimetry (DSC) was undertaken on a Q2000 DSC (TA Instruments, New Castle, DE, USA). Samples were heated from 20 – 300 °C at 10 °C $min^{-1}$, under a 40 mL $min^{-1}$ flow of $N_2$ gas. Data analysis was carried out using the TA Universal Analysis software.

### *2.3.3 X-ray diffraction*

X-ray diffraction (XRD) patterns were collected using a Miniflex 600 diffractometer (Rigaku, Tokyo, Japan). The instrument produces Cu Kα radiation at 40 kV and 15 mA; patterns were recorded in the 2Θ range 4 to 40 °C at 5° $min^{-1}$

### *2.3.4 Infrared spectroscopy*

Infrared (IR) spectroscopy was performed on a Spectrum 100 FTIR spectrometer (Perkin Elmer, Waltham, MA, USA) over the range 650 – 4000 $cm^{-1}$ and at a resolution of 1 $cm^{-1}$.

### *2.3.4 Molecular modeling*

*In vacuo* molecular mechanics calculations were performed using HyperChem version 8.0 following the methodology described in the literature (Lopez et al., 2014). In brief, the structures of the individual compounds were first drawn in ChemBioDraw Ultra 13.0. Decameric PVP and PCL oligomers were selected as representative of the polymers. These were then incorporated into HyperChem, and trial structures generated based on preset bond angles/lengths, with all hydrogen atoms explicitly included. Initial minimisations were performed using the MM+ forcefield, followed by a full energetic minimization in AMBER3. Full details may be found in our previous work (Lopez et al., 2014).

## 2.4 *In vitro* drug release assays

### *2.4.1 Preparation of the model for release studies*

The design and validation of the PK-Eye model has been previously reported (Awwad et al., 2015). Briefly, the 2-compartment model (see Figure 2) is fabricated from polyacrylate with anterior (200 µL) and posterior (4.2 mL) cavities. A washer with a Visking membrane (molecular weight cut off: 12 – 14 kDa) separates the two compartments. An inlet port into the posterior cavity near the membrane allows a ocular mimicking flow to be established through the model. An outlet port is present in the anterior cavity of the model which mimics ocular outflow and is used for continuous sampling. An injection port is present in each cavity. Aliquots can be collected from the outlet port of the anterior cavity or from the injection port of the posterior cavity.

Prior to each experiment, the model was unscrewed and a washer with a fresh Visking membrane placed inside the model. A sample (*ca.* 6 × 7 mm; mass 7.0 ± 2.1 mg (PVP) and 5.7 ± 3.4 mg (PCL)) cut from the fiber mat was placed in the posterior cavity and the model was

reassembled. For these studies, both anterior and posterior cavities of the model were filled with phosphate buffered saline (PBS; pH 7.4) through the injection port. The inlet port was connected to a 16 channel peristaltic pump and PBS flowed through the model at a flow rate of 2.0 µL $min^{-1}$. Samples were collected from the anterior chamber and filtered through a 0.22 µm filter before analysis using high-performance liquid chromatography (HPLC).

### *2.4.2 Quantification of drug release*

HPLC was used to determine the drug concentration in the aliquots collected from the PK-Eye model. A calibration curve was first constructed for each drug, and the concentrations of unknown samples were back calculated from these data. Samples from each time point were evaluated in triplicate and the mean and standard deviation (S.D.) were determined. Three independent experiments were conducted for each formulation, and the results are reported as mean ± S.D. Different HPLC methods were developed for each drug (Table 2), together with a bespoke method to permit simultaneous analysis of all three active ingredients (Tables 2 – 4). All analyses were undertaken using a Agilent 1200 series HPLC (Agilent Technologies Inc, Santa Clara, CA, USA) equipped with Chemstation software (Agilent). The rate constants ($k$) and half-life ($t_{1/2}$) of each drug were calculated by plotting the results in OriginPro. First-order kinetic rate constants ($k$) were derived from the monoexponential curve and half-lives as 0.693/$k$. The rate constants of zero-order release profiles were calculated as concentration–time and half-lives from the initial concentration [A] using [A]/2$k$.

238 **Table 2:** The HPLC conditions used to analyse drug release.

| Properties | ACY | CIP | B12 | All 3 drugs |
|---|---|---|---|---|
| **Molecular weight (g/mol)** | 225.2 | 331.3 | 1,355.3 | N/A |
| **Water solubility (mg/mL)** | 2.5 (37 °C)[a] | 6.7 (20 °C)[b] | 12.5[c] | N/A |
| **Calibration curve details** | 500 ug/mL serial diluted to 0.24 ug/mL<br>$R^2$: 0.995<br>Slope: 58.3 | 500 ug/mL serial diluted to 0.49 ug/mL<br>$R^2$: 0.991<br>Slope: 64.8 | 1000 ug/mL serial diluted to 0.49 ug/mL<br>$R^2$: 0.999<br>Slope: 6.83 | As per individual drugs |
| **Column** | Reverse phase Synergi Polar-RP Phenomenex 4 um, 15 cm column | Reverse phase Synergi Polar-RP Phenomenex 4 um, 15 cm column | Reverse phase Synergi Polar-RP Phenomenex 4 um, 15 cm column | Reverse phase Synergi Polar column 250 x 4.6 mm, 4 um, 15 cm column |
| **Wavelength (nm)** | 254 | 280 | 278 | See Table 3 |
| **Injection volume (µL)** | 10.0 | 10.0 | 10.0 | 10.0 |
| **Flow rate (mL/min)** | 1.0 | 1.0 | 1.0 | 1.0 |
| **Column temperature (°C)** | 30 | 30 | 30 | 40 |
| **Method** | Isocratic | Isocratic | Isocratic | Gradient, see Table 4 |
| **Buffers** | Buffer A: 0.1% ammonium acetate in water;<br>Buffer B: acetonitrile.<br>A:B 95:5 v/v | Buffer A: 2% aqueous acetic acid solution<br>Buffer B: acetonitrile.<br>A:B 84:16 v/v | Buffer A: 70% PBS, pH 7.4;<br>Buffer B: 30% methanol<br>A:B 70:30 v/v | Buffer A as 20 mM PBS, pH 4;<br>Buffer B: acetonitrile<br>See Tables 3-4 |
| **Retention time (mins)** | 3.1 | 4.7 | 2.13 | ACY: 6.5<br>CIP: 14.1<br>B12: 13.5 |

239 Sources: [a] http://www.drugbank.ca/drugs/DB00787; [b] hydrochloride form, (Caco et al., 2008);
240 [c] http://www.drugbank.ca/drugs/DB00115
241

242 **Table 3:** The gradient method used to analyse acyclovir, ciprofloxacin and cyanocobalamin simultaneously in HPLC.

| Time (mins) | % acetonitrile (v/v) |
|---|---|
| 0 | 5 |
| 4 | 5 |
| 10 | 40 |
| 20 | 80 |
| 20.1 | 5 |
| 25 | 5 |

243

244

**Table 4:** UV absorbance wavelengths used for the gradient method detailed in Table 3.

| Time (mins) | Wavelength (nm) |
|---|---|
| 0 | 255 |
| 11 | 360 |
| 12.75 | 279 |

# 3. Results and discussion

## 3.1 Fiber production

### *3.1.1 PVP fibers*

A range of optimization experiments were initially undertaken in which the processing parameters (voltage, polymer concentration, solvent system) were systematically varied. As a result, the conditions listed in Section 2.2 were adopted for further studies. These permitted fibers to be prepared with PVP and all three active ingredients. SEM images of the PVP systems are given in Figure 3, and details of the fiber sizes in Table 5.

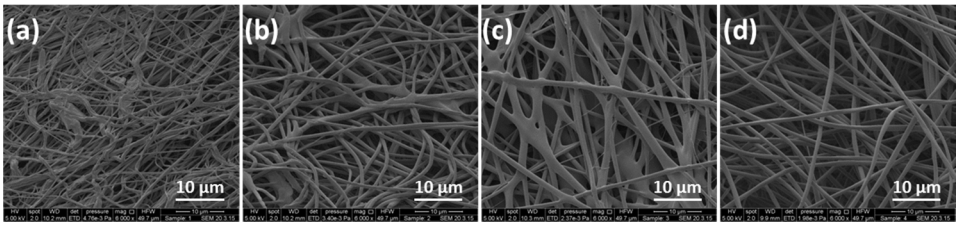


**Figure 3:** SEM images of (a) PVP-ACY; (b) PVP-CIP; (c) PVP-B12; and (d) PVP-ABC (containing all three drugs).

In all cases, cylindrical fibers can be seen to have formed. For the single-drug fibers, there is evidence for incomplete evaporation of solvent during the electrospinning process, in the form of merged fibers. However, there appears to be no significant amounts of beading present, and the PVP-ABC fibers with all three drugs having been loaded all have smooth cylindrical morphologies with no evidence of any abnormalities.

No clear trends emerge from the diameter data: there is no obvious relationship between the drug content in the fibers (PVP-ABC > PVP-ACY > PVP-CIP > PVP-B12) and their diameters (PVP-

ABC > PVP-B12 > PVP-CIP > PVP-ACY). It is presumed that both the amount of API present in solution and the effect each has on solution parameters such as viscosity and conductivity affect the diameter of the fibers obtained, thus leading to these complex patterns. Higher drug loadings appear to result in somewhat more homogenous distributions of fiber diameters.

**Table 5:** The diameters of the PVP and PCL fibers prepared.

| Fiber | Fiber diameter (nm) | Diameter uniformity (% RSD) |
|---|---|---|
| PVP-ACY | 267 ± 48 | 17.2 |
| PVP-CIP | 762 ± 159 | 20.8 |
| PVP-B12 | 921 ± 232 | 25.2 |
| PVP-ABC[a] | 932 ± 137 | 14.7 |
| PCL-ACY | 623 ± 294 | 46.9 |
| PCL-CIP | 768 ± 210 | 27.3 |
| PCL-B12 | 744 ± 267 | 35.9 |
| PCL-AC[b] | 478 ± 104 | 21.8 |
| PCL-ABC[a] | 631 ± 344 | 54.5 |

[a] Containing all three drugs; [b] containing ACY and CIP.

### *3.1.2 PCL fibers*

PCL fibers could not be formed using the chloroform and DMF solvent system used with PVP because the resultant solution was too viscous, leading to clogging of the spinneret. A range of alternatives was explored, and 1:1 v/v chloroform/methanol was found to be suitable for PCL. The fibers produced are depicted in Figure 4, and their diameters summarized in Table 5.

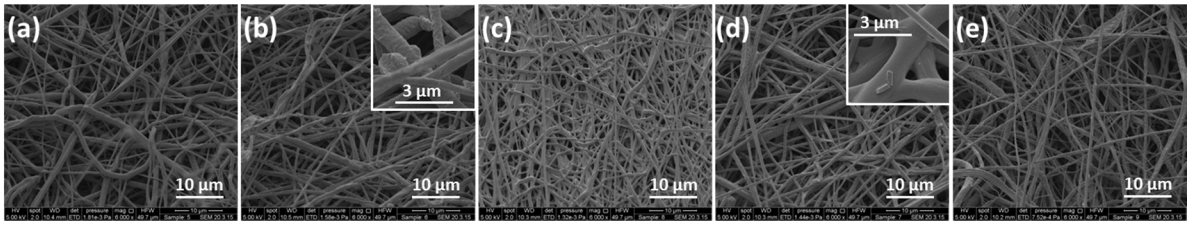


**Figure 4:** SEM images of (a) PCL-ACY; (b) PCL-CIP; (c) PCL-B12; (d) PCL-AB; and, (e) PCL-ABC

In all cases, the fibers can be seen to have cylindrical morphologies. The PCL-ACY fibers show rough and/or wrinkled surfaces in places, and high degrees of curvature. The PCL-CIP sample has similar morphology, and additionally some particles (presumably of CIP) can be seen on the

fiber surfaces (see Figure 3(b), inset). The PCL-B12 fibers are flattened owing to incomplete solvent evaporation during electrospinning. The PCL-AB fibers are smooth but again some particles can be seen on the fiber surface (Figure 3(d), inset), although these are much smaller and less frequent than those seen with PCL-CIP. PCL-ABC comprises fibers with wrinkled surfaces, presumably as a result of incomplete solvent evaporation during electrospinning. In general, the multi-drug fibers have higher quality than the single-drug systems, being virtually free of particles (a very few may be seen upon very close inspection of the PCL-AB micrographs). As before, there is no direct correlation between the fibers' API content (PCL-ABC > PCL-AC > PCL-ACY > PCL-CIP > PCL-B12) and their diameters (PCL-CIP > PCL-B12 > PCL-ABC > PCL-ACY > PCL-AC). The same is true for the diameter distributions, and the homogeneity of the fiber population cannot be directly related to the API present or the API concentration.

### 3.2 Physical form characterisation

The fiber sets were investigated using differential scanning calorimetry (DSC) and X-ray diffraction (XRD) to probe the physical form of the drug in the fibers. DSC data are presented in Figure 5.

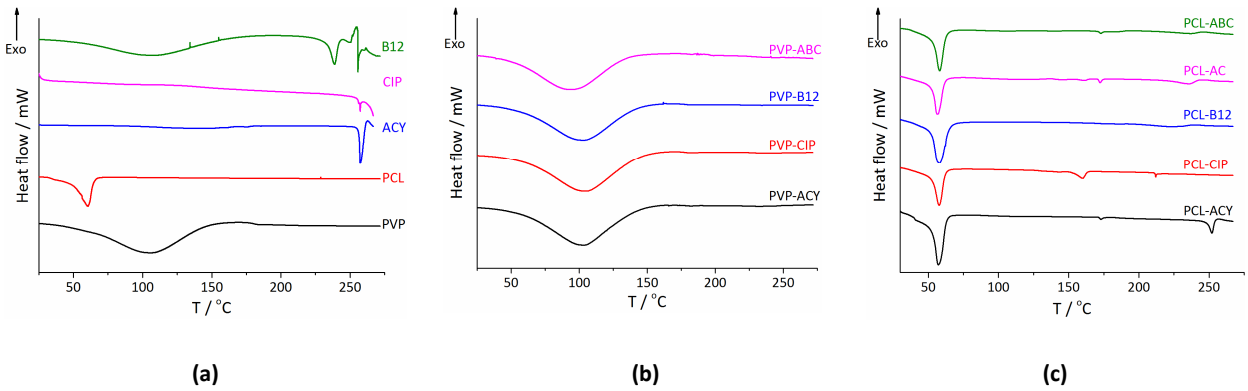


**Figure 5:** DSC data for (a) the starting materials, and electrospun fibers of (b) PVP and (c) PCL. Data have been normalised to the most intense peak in each trace for ease of comparison.

The raw polymers PVP and PCL are amorphous and semi-crystalline respectively. PVP shows a broad endotherm below 150 °C in its thermogram, corresponding to dehydration. PCL exhibits a clear melt at *ca.* 60 °C. The trace for ACY has a shallow endotherm below 175 °C, which might be attributed to dehydration, and then a melt corresponding to the most stable form II (ACY is known to exhibit complex polymorphism (Lutker et al., 2011)) is visible at *ca.* 257 °C. The latter appears to be followed by an exotherm, which might indicate degradation. CIP is also a crystalline material; melting is clearly visible at *ca.* 256 – 257 °C. The DSC data of B12 depict an endothermic peak corresponding to water loss below 150 °C and a complex series of peaks around 220 – 275 °C which are believed to correspond to degradation.

The drug-loaded PVP fibers are all amorphous: the only distinct features in the DSC traces are broad endotherms corresponding to the loss of water. No melting events can be seen. Considering the PCL systems, in all cases, the PCL melting endotherm is present at *ca.* 57 – 58 °C, reduced slightly from the pure polymer value as a result of the plasticizing influence of the small-molecule APIs incorporated. A close inspection of all the DSC traces for the PCL fibers suggests traces of crystallinity are present (see Figure 5(c)); a particularly marked endothermic peak is present for the ACY fibers at 252 °C, indicating the possible presence of form VI of ACY (Lutker et al., 2011).

To investigate further the physical form of the drug in the fibers, X-ray diffraction (XRD) measurements were undertaken (see Figure 6). The CIP and ACY starting materials are evidently crystalline, while B12 is amorphous. PVP is also amorphous, and PCL is semi-crystalline is nature. These observations all concur with the literature. The PVP fibers largely appear to contain the drug in the amorphous physical form, as proven by a lack of Bragg reflections in the patterns. For PVP-ABC however, there is evidence for some crystalline

material present, with small Bragg reflections (believed to correspond to ACY) clearly visible between 20 and 30°. The XRD patterns of the PCL fibers show the distinctive reflections of PCL, with some additional peaks also visible. These are few and low intensity, meaning that the nature of these is not completely clear, but those in PCL-ABC correspond closely to those of the ACY raw material. In any case, it is clear that some crystalline material is present, in good agreement with the DSC data.

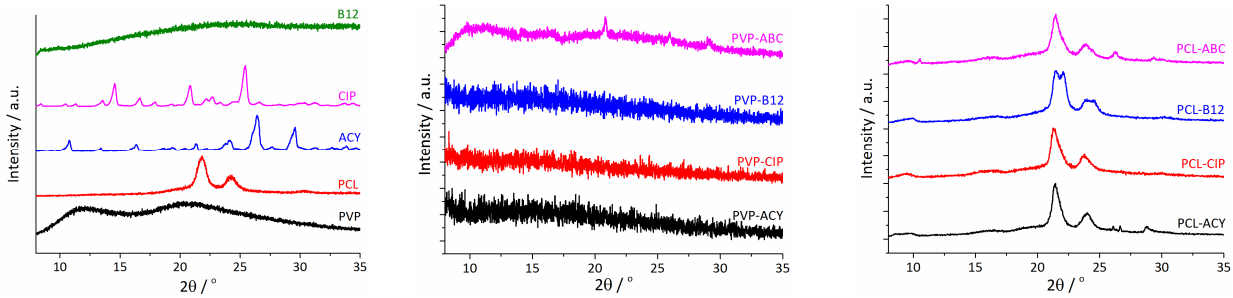


**Figure 6:** XRD patterns for (a) the starting materials, and the fibers of (b) PVP and (c) PCL produced. The intensities have been normalised to the most intense reflection in each pattern for ease of comparison.

## 3.3 Drug-polymer interactions

The interactions between the drug and polymer were investigated using both IR spectroscopy and molecular modelling.

### *3.3.1 IR spectroscopy*

IR spectra of the raw materials and fibers are presented in Figure 7.

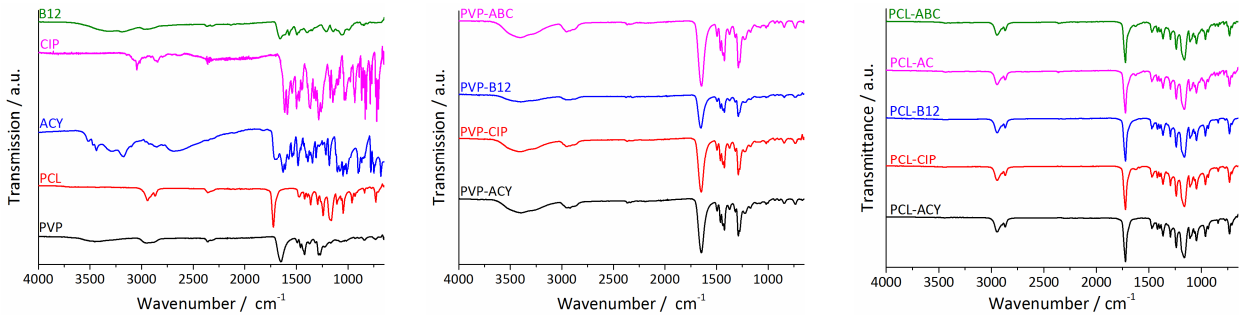


**(a)** **(b)** **(c)**

**Figure 7:** IR spectra for (a) the starting materials, and electrospun fibers of (b) PVP and (c) PCL.

An inspection of the data in Figure 7 reveals the IR spectra of the fibers to be dominated by the features of the polymer carrier. The spectra in Figure 7(b) are indistinguishable from that of PVP, and similarly those in Figure 7(c) show no significant differences from the PCL spectrum. This is not surprising given that the diagnostic vibration bands for the APIs occur over the same wavenumber range as those of the polymers (see Figure 7(a)), and also in many cases the drug loading is low (< 5 % w/w). As a result, it is not possible to say from these data whether there are any interactions between the APIs and polymers, although from their chemical structures it is thought that such interactions are likely to arise. To probe these possibilities in more detail, simple molecular models were constructed.

### *3.3.2 Molecular modeling*

To evaluate the interactions between the drug molecules and the polymer in the fibers, molecular models of the APIs and polymers and the various combinations of drug and polymer were constructed using the HyperChem software. A PVP or PCL decamer (10-mer) were taken as representative of the polymers, and both these structure and those of the APIs were optimized. Suitable combinations of the energetically minimized structures were merged to create drug-polymer complexes. The drug-polymer composites were then themselves minimized, with the results shown in Figure 8.

The energetic contributions to the overall steric energy for both the drug-polymer complexes and the individual API and PVP or PCL decamers are presented in Table 6. Stabilization of the complexes is indicated by a negative difference (ΔE) between the total steric energy of the complex and the sum of the total steric energies of the individual molecules. The data reveal that all the drug/polymer complexes have negative ΔE values, demonstrating the possibility for favorable secondary interactions to occur between the fiber components. The ΔE values for the PVP systems are more negative than those with PCL, suggesting stronger interactions arise in the former case.

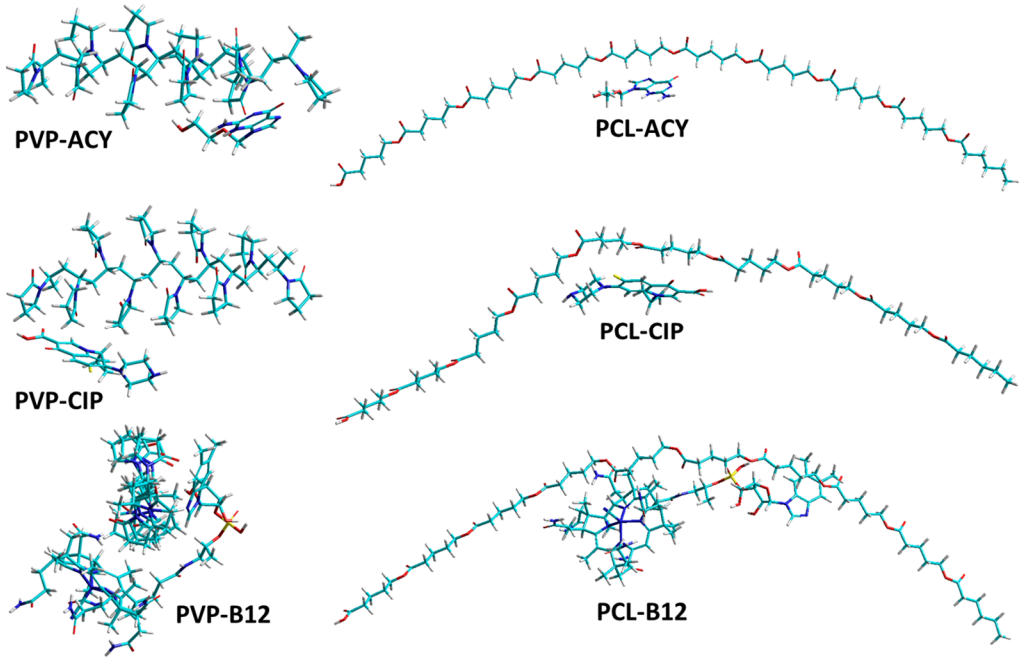


**Figure 8:** Energy minimized structures of the polymer-drug complexes. The polymer is at the top of each image, and the drug at the bottom.

382 **Table 6:** The energetics of the optimized geometries in the polymer-drug complexes.

| System | Minimised energy contributions / kcal mol$^{-1}$ | | | | | | |
|---|---|---|---|---|---|---|---|
| | Bond stretching | Bond angle | Torsional | van der Waals | H-bonding | ΣE | ΔE |
| ACY | 0.296 | 3.150 | 1.002 | 1.172 | -0.051 | 5.569 | - |
| CIP | 0.988 | 99.988 | 9.139 | 8.057 | -0.006 | 118.166 | - |
| B12 | 7.047 | 174.957 | 58.893 | 0.739 | -0.301 | 241.336 | - |
| PVP | 4.337 | 82.689 | 46.017 | -12.788 | 0.000 | 120.255 | - |
| PCL | 0.675 | 2.911 | 0.012 | 8.780 | 0.000 | 12.378 | - |
| PVP-ACY | 4.550 | 84.337 | 47.984 | -24.382 | -0.094 | 112.395 | -13.429 |
| PVP-CIP | 5.137 | 179.346 | 56.773 | -17.580 | -0.006 | 223.669 | -14.753 |
| PVP-B12 | 11.688 | 257.214 | 103.517 | -39.641 | -1.036 | 331.742 | -29.848 |
| PCL-ACY | 0.922 | 6.304 | 1.100 | 2.305 | -0.136 | 10.496 | -7.451 |
| PCL-CIP | 1.547 | 102.621 | 10.114 | 2.693 | -0.039 | 116.936 | -13.609 |
| PCL-B12 | 9.844 | 177.507 | 55.995 | -11.361 | -0.412 | 231.573 | -22.141 |

383

384 ### 3.4 Drug release

385 All experiments were performed using PBS (pH 7.4) as a vitreous substitute in the PK-Eye model
386 to permit time-efficient screening of the various formulations. Samples were taken from the
387 anterior cavity outflow, and the drug concentrations in these aliquots were used to calculate
388 the content in the posterior cavity. A steady state condition is established relatively quickly for
389 low molecular weight drugs so the solution drug concentrations are the same in both cavities.
390 This assumption has been validated in a previous study (Awwad et al., 2015). The release data
391 from the single drug-loaded fibers are given in Figure 9, and a summary of the calculated
392 parameters for all the fibers can be found in Table 7.

393

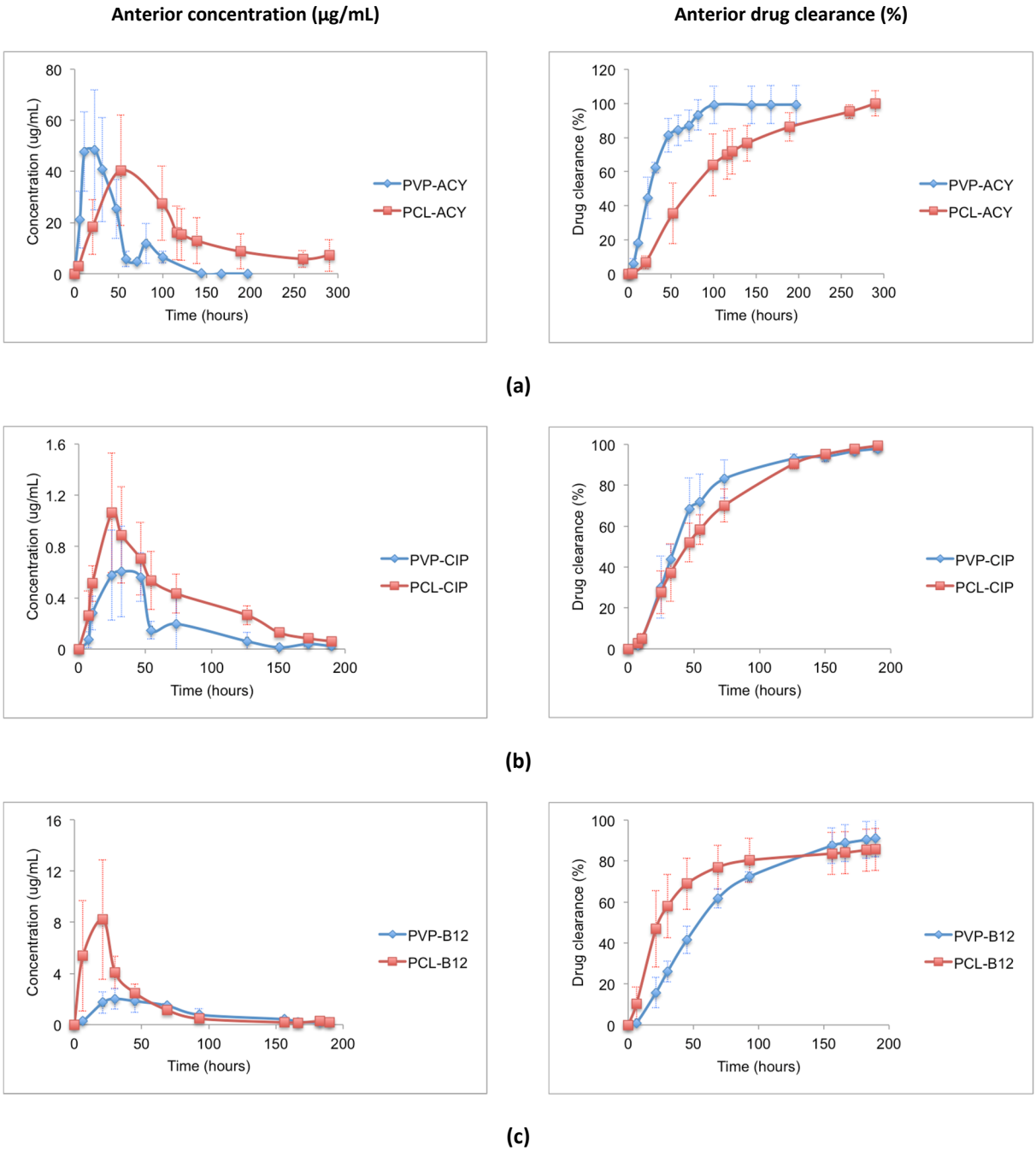


394 **Figure 9**: Release kinetics of PVP and PCL fibers loaded with (a) ACY, (b) CIP, and (c) B12 in the PK-Eye. All results are displayed
395 as mean ± S.D. from three independent experiments. The anterior drug concentration is shown on the left, and the drug
396 clearance on the right.

397

398 *3.4.1 ACY release*

399 ACY is a potent systemic antiviral that is used for acute retinal necrosis because of its selectivity
400 against the herpes simplex virus and the varicella-zoster virus. Direct ocular application has
401 been found to be beneficial in controlling this type of aggressive retinitis within the first 48

hours, when systemic ACY has not reached the required therapeutic levels in the retina (Damico et al., 2012). Intravitreal anti-virals have been used since the early 1990s for the treatment of CMV and have also been used in acute retinitis necrosis (Tam et al., 2012). The intravitreal delivery of acyclovir is safe and well tolerated by rabbit retina, but its half-life *in vivo* is short (Damico et al., 2012; John, 2007; Peyman et al., 2008).

When the ACY loaded PVP fibers were tested in the PK-Eye, the drug concentration displayed a mono-exponential decrease following first order kinetics (Figure 9(a)). The fibers led to an ACY residence time of 0.95 ± 0.12 days with a maximum concentration of 48.5 ± 23.5 μg/mL observed after 23 hours. The PCL-ACY fibers gave a residence time of 3.67 ± 1.4 days, with the highest concentration of 40.4 ± 21.6 μg/mL seen after 88 h. When other anti-viral drugs (*e.g.* ganciclovir) were tested in the preliminary stages of PK-Eye development, their half-life was seen to be only a few hours (data not shown) which is consistent with human and animal data. Once in solution, low molecular weight drugs are eliminated quickly from the human eye and this is seen in the model. The data indicate the fibers prolong the release of acyclovir over 1 – 4 days. For both sets of materials, around 70 – 80 % of the theoretical loading is released. PVP is more soluble than PCL in water, and thus might be expected to give much more rapid drug release. However, in the PK-Eye model, the small volumes and flow rates involved mean that the dissolution of PVP is slow, and it is to be presumed that a balance of polymer solubility and the strength of the polymer/drug interactions (the latter are stronger for PVP) influence the release kinetics.

### *3.4.2 CIP release*

CIP has a wide spectrum of anti-Gram negative bactericidal activities and has been used in the treatment of many clinical infections (Hui et al., 2004). It is considered effective for the

treatment of intraocular infections and prophylaxis, and has also been found to be non-toxic to rabbit retina (Peyman et al., 2008). CIP has a molecular weight of 331.3 g/mol, and a terminal half-life of 4 – 5 days in rabbit eyes has been reported (Haghjou et al., 2013; Liu et al., 1998; Peyman et al., 2008). However, other studies report a half-life of 2.2 hours and 1 hour in normal and aphakic eyes (from which the lens has been removed) respectively (Pearson et al., 1993). Similar to ACY, CIP has poor water solubility at low pH. It is almost insoluble in neutral pH, while its solubility increases with increasing pH value (approximately 30 mg/mL at pH 11).

Both the PVP-CIP and PCL-CIP fibers showed prolonged half-lives, with CIP clearance following first order kinetics (Figure 9(b)). PVP-CIP displayed an ocular residence time of approximately 1.36 ± 0.4 days, with the highest drug concentration reaching 0.61 ± 0.35 μg/mL at 32 hours. It took about 190 hours (approx. 8 days) for no drug to be detectable in the outflow liquid by HPLC. PCL-CIP showed a slight extension of half-life as compared to PVP-CIP, with a residence time of 2.1 ± 0.68 days. The highest concentration observed was 1.06 ± 0.47 μg/mL at 24 hours and after around 190 hours release no further release was seen. Only 3.5 – 4 % of the theoretical loading was seen to be released with both polymers. This can perhaps be ascribed to the low solubility of CIP at pH 7.4, and the strong interactions between this API and both PVP and PCL indicated by molecular modelling. As for with ACY, we believe that a balance of drug and polymer solubility and drug/polymer interactions govern the release process.

### *3.4.3 B12 release*

Deficiencies of cyanocobalamin, vitamin B12, have been connected with burning pain and foreign body sensations in the eyes (Shetty et al., 2015) and visual acuity (Doan and Chao, 2014). B12 is also used in some eye drops (Santen Pharmaceutical Co, 2013). The PVP-B12 and PCL-B12 fibers (Figure 9(c)) presented the highest concentration of drug after around 30 hours

(2.01 ± 0.79 µg/mL) and 21 hours (8.21 ± 4.7 µg/mL) respectively. B12 clearance from PK-Eye with both sets of fibers followed first order kinetics, with a mono-exponential decrease. PVP-B12 had a slightly slower rate of release than PCL-B12, with observed residence times of 2.32 ± 0.78 days and 0.80 ± 0.21 days respectively. This can possibly be ascribed to the stronger drug/polymer interactions calculated with PVP. Around 25% of the theoretical loading was released into solution.

### *3.4.4 Multidrug systems*

The PCL-ABC fibers were also tested in the PK-Eye (Figure 10). The highest concentrations of ACY, B12 and CIP detected in the model were around 39.7 ± 2.4 µg/mL (17 hours), 14.3 ± 1.9 µg/mL (17 hours) and 3.6 ± 0.12 µg/mL (208 hours) respectively. With these fibers, both ACY and B12 release followed first order kinetics while CIP followed zero order kinetics. The residence times for ACY, B12 and CIP were 1.4 ± 0.08 days, 6.16 ± 0.6 days and 2.99 ± 0.19 days. In terms of the theoretical loading, *ca.* 33 %, 50 % and 100 % of ACY, CIP, and B12 were released respectively. The PCL-ABC fibers release a greater percentage of their B12 and CIP loadings than the single-drug analogues, but rather less of the ACY loading. The percentages released correlate with the API solubilities (B12 > CIP > ACY), but inversely with the strength of interactions between the API and PCL. The reasons for this are not entirely clear, but it may be that the presence of multiple APIs in the fibers diminishes the importance of the PCL/API interactions and causes the solubility factor to become dominant in determining the amount released.

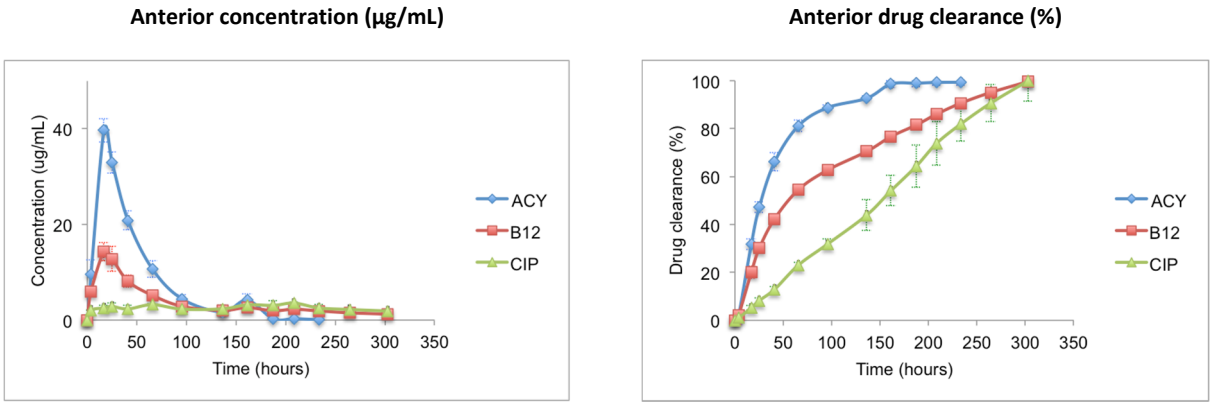


**Figure 10**: Drug release kinetics from (a) PVP-ABC and (b) PCL-ABC in the PK-Eye. All results are displayed as mean ± S.D. from three independent experiments.

**Table 7:** A summary of the kinetic parameters determined using the PK-Eye model.

| System | | Cumulative mass released (µg) | Rate constant ($h^{-1}$) | Half-life (d) | % of theoretical loading released |
|---|---|---|---|---|---|
| PVP-ACY | | 248.4 ± 27.7 | 0.031 ± 0.004 | 0.95 ± 0.12 | 71.0 |
| PVP-CIP | | 3.82 ± 0.05 | 0.022 ± 0.008 | 1.36 ± 0.4 | 3.51 |
| PVP-B12 | | 19.1 ± 1.9 | 0.014 ± 0.005 | 2.32 ± 0.8 | 26.2 |
| PCL-ACY | | 543.7 ± 40.4 | 0.009 ± 0.004 | 3.67 ± 1.4 | 81.7 |
| PCL-CIP | | 8.15 ± 0.1 | 0.015 ± 0.005 | 2.02 ± 0.7 | 3.75 |
| PCL-B12 | | 34.3 ± 4.1 | 0.038 ± 0.010 | 0.80 ± 0.2 | 23.3 |
| PCL-ABC | ACY | 208.7 ± 12.4 | 0.021 ± 0.02 | 1.4 ± 0.08 | 33.2 |
| | CIP | 94.0 ± 8.01 | 0.32 ± 0.03 | 6.16 ± 0.6 | 49.8 |
| | B12 | 125.6 ± 0.8 | 0.01 ± 0.0006 | 2.99 ± 0.19 | 99.9 |

## 4. Conclusions

Two series of electrospun fibers were successfully prepared for ocular drug delivery applications. These were loaded with the acyclovir, ciprofloxacin, and cyanocobalamin, or combinations of these active ingredients. One set of fibers was prepared with poly(vinylpyrrolidone) (PVP) and the other with poly(caprolactone) (PCL). The fibers formed had generally cylindrical morphologies, although there was some evidence of residual solvent being present in the PVP systems, and for drug particles in the case of PCL. The PVP fibers appeared to contain the drug in the amorphous physical form, while some crystalline nature was retained in the PCL materials. The active ingredients and polymers can form favourable intermolecular

bonds when combined. Drug release studies were performed in a representative *in vitro* model of the eye, and the fiber formulations found to result in half-lives of up to 6 days. These are much greater than those of pure small molecule drug solutions in the same model, thus suggesting that the strategy adopted in this work is a viable one for the generation of intravitreal implants.

## 5. Acknowledgements

AB thanks the Russian Government for the award of a Presidential Scholarship permitting her to study at UCL. JJQ would like to thank the University of Alcalá for the award of a grant in the Research Training Framework, and SA gratefully acknowledges funding from the UCL Overseas Research Student Fund. We are further thankful for funding from: the National Institute of Health Research (NIHR) Biomedical Research Centre at Moorfields Eye Hospital NHS Foundation Trust and UCL Institute of Ophthalmology; Moorfields Special Trustees; the Helen Hamlyn Trust (in memory of Paul Hamlyn); the Medical Research Council; Fight for Sight; and, the Freemasons Grand Charity. S.B. is grateful for funding from the UK Engineering & Physical Sciences Research Council (EPSRC) for the EPSRC Centre for Innovative Manufacturing in Emergent Macromolecular Therapies (EP/I033270/1). Financial support from the consortium of industrial and governmental users for the EPSRC Centre is also acknowledged. Finally, we thank Mr John Frost for all his advice and help to fabricate prototypes of the PK-Eye and Mr David McCarthy for SEM images.

## 6. References

Awwad, S., Lockwood, A., Brocchini, S., Khaw, P.T., 2015. The PK-Eye: A novel in vitro ocular flow model for use in preclinical drug development. J. Pharm. Sci. 104, 3330-3342.

Bottino, M.C., Arthur, R.A., Waeiss, R.A., Kamocki, K., Gregson, K.S., Gregory, R.L., 2014. Biodegradable nanofibrous drug delivery systems: Effects of metronidazole and ciprofloxacin on periodontopathogens and commensal oral bacteria. Clin. Oral Invest. 18, 2151-2158.

517 Caco, A.I., Varanda, F., Pratas de Melo, M.J., Dias, A.M.A., Dohrn, R., Marrucho, I.M., 2008.
518 Solubility of antibiotics in different solvents. 1. Hydrochloride forms of tetracycline,
519 moxifloxacin, and ciprofloxacin. Ind. Eng. Chem. Res. 47, 8083-8089.

520 Chakraborty, S., Liao, I.C., Adler, A., Leong, K.W., 2009. Electrohydrodynamics: A facile
521 technique to fabricate drug delivery systems. Adv. Drug Del. Rev. 61, 1043-1054.

522 Chen, H.-M., Yu, D.-G., 2010. An elevated temperature electrospinning process for preparing
523 acyclovir-loaded PAN ultrafine fibers. J. Mater. Process. Tech. 210, 1551-1555.

524 Damico, F.M., Scolari, M.R., Ioshimoto, G.L., Takahashi, B.S., Cunha-Jr, A.S., Fialho, S.L., Bonci,
525 D.M., Gasparin, F., Ventura, D.F., 2012. Vitreous pharmacokinetics and electroretinographic
526 findings after intravitreal injection of acyclovir in rabbits. Clinics 67, 931-937.

527 Doan, T., Chao, J.R., 2014. A woman with bilateral maculopathy and acquired vitamin B12
528 deficiency. Eye 28, 905-906.

529 El-Shanshory, A.A., Chen, W., El-Hamshary, H.A., Al-Deyab, S.S., Mo, X., 2015. Antibacterial
530 ciprofloxacin hydrochloride incorporated PVA/regenerated silk fibroin nanofibers composite for
531 wound dressing applications. J. Controlled Release 213, E8-E9.

532 Haghjou, N., Abdekhodaie, M.J., Cheng, Y.-L., 2013. Retina-choroid-sclera permeability for
533 ophthalmic drugs in the vitreous to blood direction: quantitative assessment. Pharm. Res. 30,
534 41-59.

535 Hui, M., Kwok, A.K.H., Pang, C.P., Cheung, S.W., Chan, R.C.Y., Lam, D.S.C., Cheng, A.F.B., 2004.
536 An in vitro study on the compatibility and precipitation of a combination of ciprofloxacin and
537 vancomycin in human vitreous. Br. J. Opthalmol. 88, 218-222.

538 John, B., 2007. Intravitreal injections. Kerala J. Ophthalmology 200, 46-57.

539 Jouan, M., Katlama, C., 1999. Management of CMV retinitis in the era of highly active
540 antiretroviral therapy. Int. J. Antimicrob. Agents 13, 1-7.

541 Kuno, N., Fujii, S., 2011. Recent advances in ocular drug delivery systems. Polymers 3, 193-221.

542 Liu, W., Feng, Q., Perkins, R., Drusano, G., Louie, A., Madu, A., Mian, U., Mayers, M., Miller,
543 M.H., 1998. Pharmacokinetics of sparfloxacin in the serum and vitreous humor of rabbits:
544 Physicochemical properties that regulate penetration of quinolone antimicrobials. Antimicrob.
545 Agents Chemother. 42, 1417-1423.

546 Liu, Z.P., Cui, L., Yu, D.G., Zhao, Z.X., Chen, L., 2014. Electrosprayed core-shell solid dispersions
547 of acyclovir fabricated using an epoxy-coated concentric spray head. Int. J. Nanomedicine 9,
548 1967-1977.

549 Lopez, F.L., Shearman, G.C., Gaisford, S., Williams, G.R., 2014. Amorphous formulations of
550 indomethacin and griseofulvin prepared by electrospinning. Mol. Pharm. 11, 4327-4338.

551 Lutker, K.M., Quinones, R., Xu, J., Ramamoorthy, A., Matzger, A.J., 2011. Polymorphs and
552 hydrates of acyclovir. Journal of pharmaceutical sciences 100, 949-963.

553 Macocinschi, D., Filip, D., Vlad, S., Cernatescu, C., Tuchilus, C.G., Gafitanu, C.A., Dumitriu, R.P.,
554 2015. Electrospun/electrosprayed polyurethane biomembranes with ciprofloxacin and clove oil
555 extract for urinary devices. J. Bioact. Compat. Polym. 30, 509-523.

556 Pearson, P.A., Hainsworth, D.P., Ashton, P., 1993. Clearance and distribution of ciprofloxacin
557 after intravitreal injection. Retina 13, 326-330.

558 Peyman, G.A., Lad, E.M., Moshfeghi, D.M., 2008. Intravitreal injection of therapeutic agents. .
559 Retina 29, 875-912.

560 Pollard, R., 1996. CMV retinitis: ganciclovir/monoclonal antibody. Antiviral Res. 29, 73-75.

561 Santen Pharmaceutical Co, L., 2013. http://www.santen.com/en/news/20130509.pdf.

562 Shetty, R., Deshpande, K., Ghosh, A., Sethu, S., 2015. Management of ocular neuropathic pain
563 with Vitamin B12 supplements: A case report. Cornea 34, 1324-1325.

564 Short, B., 2008. Safety evaluation of ocular drug delivery formulations: techniques and practical
565 considerations. Tox. Path. 36, 49-62.

566 Song, F., Wang, X.L., Wang, Y.Z., 2011. Poly (N-isopropylacrylamide)/poly (ethylene oxide) blend
567 nanofibrous scaffolds: thermo-responsive carrier for controlled drug release. Colloids Surf. B 88,
568 749-754.

569 Tam, P.M.K., Hooper, C.Y., Lightman, S., 2012. Antiviral selection in the management of acute
570 retinal necrosis. Clin. Ophthalmol. 4, 11-20.

571 Unnithan, A.R., Barakat, N.A.M., Pichiah, P.B.T., Gnanasekaran, G., Nirmala, R., Cha, Y.-S., Jung,
572 C.-H., El-Newehy, M., Kim, H.Y., 2012. Wound-dressing materials with antibacterial activity from
573 electrospun polyurethane-dextran nanofiber mats containing ciprofloxacin HCl. Carbohydrate
574 Polym. 90, 1786-1793.

575 Williams, G.R., Chatterton, N.P., Nazir, T., Yu, D.-G., Zhu, L.-M., Branford-White, C.J., 2012.
576 Electrospun nanofibers in drug delivery: recent developments and perspectives. Therap. Del. 3,
577 515-533.

578 Yu, D.-G., Branford-White, C., Li, L., Wu, X.-M., Zhu, L.-M., 2010. The compatibility of acyclovir
579 with polyacrylonitrile in the electrospun drug-loaded nanofibers. J. Appl. Polym. Sci. 117, 1509-
580 1515.

581 Yu, D.G., Zhu, L.M., Branford-White, C.J., Yang, J.H., Wang, X., Li, Y., Qian, W., 2011. Solid
582 dispersions in the form of electrospun core-sheath nanofibers. Int. J. Nanomedicine 6, 3271-
583 3280.

584